JOURNAL OF CATALYSIS 98, 264–276 (1986)

Structure and Reactivity of Alumina-Supported Iron Catalysts for Ammonia Synthesis

J. E. SUEIRAS,*,[1] N. HOMS,* P. RAMIREZ DE LA PISCINA,* M. GRACIA,† AND J. L. G. FIERRO‡,[1]

*Departamento de Química Inorgánica, Facultad de Química, Pl. Imperial Tarraco, 39005 Tarragona; †Instituto de Química-Física "Rocasolano," CSIC, Serrano 119, 28006 Madrid; and ‡Instituto de Catálisis y Petroleoquímica, CSIC, Serrano 119, 28006 Madrid, Spain

Received July 16, 1985; revised October 18, 1985

Alumina-supported iron catalysts, obtained either by impregnation of iron from a $K_4[Fe(CN)_6]$ aqueous solution upon several acid-modified γ-Al_2O_3 samples or by the incipient wetness method, were characterized and their activities for ammonia synthesis at atmospheric pressure and 593 K were studied. Characterization was carried out by temperature-programmed reduction (TPR), kinetics of hydrogen reduction, CO chemisorption, X-ray photoelectron spectroscopy (XPS), IR spectroscopy, and Mössbauer spectroscopy, resulting in the degree of reduction and the dispersion of the metallic phase dependent on the previous acid modification of the γ-Al_2O_3. The XPS surface composition expressed as M 2*p*/Al 2*p* (M = Fe, K) gave K 2*p*/Al 2*p* > Fe 2*p*/Al 2*p*. IR experiments, with NO as probe molecule, exhibited bands for reduced catalysts at 1778 and 1712 cm^{-1} whose intensity and position depended on the protonation degree of γ-Al_2O_3 and promoter content, respectively. Mössbauer spectra of the reduced samples showed the presence of surface α-Fe, superparamagnetic Fe^0, Fe^{2+}, Fe^{3+}, and α-Fe_2O_3 depending on the catalyst. Finally, the catalytic activity for ammonia synthesis was found to be dependent on the surface structure of the catalyst and hence on the method of preparation.

INTRODUCTION

Catalysts prepared from supported and unsupported Group VIII metals are commonly used in the ammonia synthesis reaction (*1–4*). The low concentration of the active phase present in supported catalysts, when compared with those of industrial counterparts, facilitates the study and understanding of stability, dispersion, and other characteristics of the active phase, in ammonia synthesis catalysts. Modification of γ-alumina properties (*5–7*) and different methods of impregnation (*8, 9*) were reported. Recently, we described a method for acid modification of γ-alumina (*10*), and we reported the preparation, characterization, and catalytic activities of supported iron and ruthenium catalysts for ammonia synthesis at atmospheric pressure (*11–16*).

In this work we studied the preparation of catalysts from iron supported on acid-modified γ-alumina; their characterization using temperature-programmed reduction (TPR) measurements; kinetics of hydrogen reduction; CO chemisorption; X-ray photoelectron spectroscopy (XPS), IR spectroscopy, and Mössbauer spectroscopy; and finally their catalytic activity for ammonia synthesis at atmospheric pressure and 593 K, correlating the catalytic activity with surface properties and method of preparation.

EXPERIMENTAL

Catalyst Preparation

Several samples of Girdler γ-alumina with a BET surface area of 188 $m^2 g^{-1}$ and a pore volume of 0.39 $cm^3 g^{-1}$ were acid-modified as reported elsewhere (*11–13*). These samples were labeled NA, PA1, PA2.5, PA5, PA10, and PA20 corresponding to the amount of H^+ [mmole H^+ (g γ-Al_2O_3)$^{-1}$]

[1] To whom correspondence may be sent.

0021-9517/86 $3.00

added to the solution: 0, 1.0, 2.5, 5.0, 10.0, and 20.0, respectively. The acid site content of the samples was determined by UV spectrophotometry, as reported in the literature (*10*), with prior filtration and drying under vacuum at 393 K for 12 h.

Samples (3.75 g) of the filtered and dried acid-modified support were impregnated with 50 cm^3 of a 0.32 *M* $K_4[Fe(CN)_6]$ aqueous solution stirred for 1.5 h. Two nonmodified alumina samples were also impregnated with aqueous solutions of $K_4[Fe(CN)_6]$ and $Fe(NO_3)_3 \cdot KNO_3$ by the incipient wetness method, resulting in catalysts that contained 3.2% Fe (labeled 3IW) and 15% Fe (labeled 15IW), respectively. Impregnated samples were filtered off, dried at 333 K, and calcined up to 873 K under an air flow for 24 h. Reduction was carried out in a tubular reactor with a $H_2 : N_2$ (3 : 1) flow rate increasing up to 100 $cm^3\ min^{-1}$ and temperature increasing up to 773 K for 72 h.

Catalyst Characterization

Iron analysis. Iron content of the catalysts was determined by flame atomic absorption spectrometry using an IL 551 spectrometer.

Reduction measurements. The reduction kinetics of catalysts were measured in a Cahn RG microbalance connected to a high-vacuum line and a gas-handling system. Samples (250 mg) were outgassed at 773 K until a constant weight was reached and then were exposed to 40 kN m^{-2} H_2. As water readsorption on the carrier is negligible at this temperature, the weight change of the catalysts with time was taken as the extent of the reduction, α_t, which was determined as the ratio of experimental weight loss to theoretical weight loss expected for the total reduction of Fe_2O_3 to metallic Fe. Initial reduction rates were calculated by analytical differentiation at zero time of the integral data fitted to a mathematical equation. Reduction experiments at programmed temperature were conducted in the same gravimetric system. Samples (40 mg), outgassed at 823 K for 12 h and then cooled to room temperature, were exposed to 40 kN m^{-2} H_2 and subsequently heated to 1100 K, at 4 K min^{-1}.

CO chemisorption. CO chemisorption was performed according to Emmett and Brunauer's recommendations (*18–20*). A 250-mg precursor was reduced in hydrogen (40 kN m^{-2}) at 770 K for 35 h. After reduction, the sample was evacuated to 1.3×10^{-4} N m^{-2} for 2 h at 770 K and cooled to room temperature, before the first CO isotherm was taken. Evacuation to 1.3 N m^{-2} for 0.2 h at room temperature followed the first isotherm, and a second isotherm was then recorded. CO was previously purified by slow passage through a 4-Å molecular sieve–charcoal train, condensed in a trap at 77 K, and then distilled to a 4-dm^3 reservoir.

X-Ray photoelectron spectra. XPS spectra were acquired with a Vacuum Generator ESCA 3 spectrometer equipped with a magnesium anode (MgK_α = 1253.6 eV), operated at 14 kV and 20 mA. A Tracor Norther TN-1710 signal averager allowed accumulation of spectra until a desired signal-to-noise ratio was reached. The analysis energy was fixed at 50 eV. Residual pressure inside the analysis chamber was better than 1×10^{-6} N m^{-2}. The powdered samples were pressed (4×10^4 kN m^{-2}) and then mounted on holders fixed on a long rod which allowed a rapid entry into the analysis chamber. C 1*s*, O 1*s*, Al 2*p*, K 2*p*, and Fe 2*p* signals were recorded for each catalyst. All binding energies (BE) were referred to the C 1*s* line at 285.0 eV.

Infrared spectra. For infrared experiments, the catalysts were ground to a fine powder and pressed at 1.3×10^4 kN m^{-2} into a 1.2-cm-diam wafer. These wafers were placed in a special vacuum cell assembled with greaseless stopcocks and NaCl windows, which allowed thermal treatments either under vacuum or on flowing gases. Pretreatment of the catalyst consisted of heating at 723 K for 2 h in a dynamic high vacuum ($\sim 1.3 \times 10^{-3}$ N m^{-2})

and/or reducing in a H_2 flow (7.2 dm^3 STP h^{-1}) and then evacuation at 723 K for 2 h. Infrared spectra were obtained with a Perkin–Elmer 580B spectrophotometer interfaced to a data system. Good-quality spectra were obtained after several accumulations and subsequent smoothing. All spectra were obtained in the double-beam mode, with a fixed slitwidth which was adjusted according to sample opacity. Nitric oxide (99.5% volume) was purified by three freeze–pump–thaw cycles, and then the distillate was collected in a 4-dm^3 ball. Hydrogen (99.98% volume) was purified by passage through a Deoxo purifier.

Mössbauer spectrometry. A conventional Mössbauer spectrometer operating in the constant acceleration mode was used. All spectra were taken at room temperature, working in the transmission mode with a ^{57}Co (Pd) source. The spectra were computer-fitted to a sum of Lorentzian-shaped lines. The goodness of fit was monitored by the χ^2 test. Mössbauer data in Tables 1 and 2 correspond to the fitted parameters.

Catalytic Activity

Synthesis and detection of ammonia. Ammonia synthesis reaction was performed at atmospheric pressure in a 100-cm^3 close recirculating system equipped with a descending-flow tubular microreactor, peristaltic pump, gas/vacuum inlets, etc. Before the reaction step all catalysts were pretreated with N_2 for 6 h at 593 K. The reaction conditions were total pressure = 101.3 kN m^{-2}, temperature = 593 K, feed H_2/N_2 = 3/1 mole, reaction time = 24 h, and catalyst samples = about 2 g.

Reactants and products were bubbled through a cold trap containing distilled water. The ammonia formed during the reaction and regained in this solution was titrated by Chaney and Marbach's method (*17*).

RESULTS AND DISCUSSION

Catalyst Structure

Catalyst reduction. Reduction of the catalysts was carried out gravimetrically, in an H_2 atmosphere, in two different ways: reduction at programmed temperature (TPR), and kinetics of reduction at constant temperature (520°C).

TPR results are depicted in Table 1 for the alumina-supported iron catalysts in the temperature range 25–840°C. This table includes TPR results for catalysts prepared from nonprotonated γ-alumina (NA), protonated γ-alumina (PA), and γ-alumina prepared by the incipient wetness method (3IW), for comparative purposes. Only at higher temperatures (750–850°C) are catalysts reduced quantitatively to Fe^0. Table 1 shows that the 3IW sample starts to be

TABLE 1

Chemical Composition and Reducibility of Fe/Al_2O_3 Catalysts

Catalyst	% K	% Fe	T_0(°C)[a]	r_0 [mg (g Fe)$^{-1}$ min^{-1}]	α_f(%)[b]
NA	6.4	2.3	365	11.9	59.1
PA1	7.3	2.6	365	10.1	57.4
PA2.5	7.8	2.8	365	8.8	55.0
PA5	8.4	3.0	365	32.3	61.9
PA10	8.8	3.1_5	365	29.6	63.0
PA20	9.5	3.4	365	27.9	39.4
3IW	8.9_5	3.2	335	35.6	63.7

[a] Temperature at which reduction (TPR profiles) starts.
[b] Reduction degree determined after 16 h.

reduced at a temperature slightly lower (335°C) than those of the NA and PA samples (365°C). This fact suggests that the impregnation method used must be responsible for the different species with different reducibility at the interface. In fact, the dispersion degrees obtained from the NA and PA samples, impregnated from a stirred suspension until equilibrium of adsorption (*13*) (called "free adsorption" samples hereon) was reached, are higher than those of the "incipient wetness" samples (Table 2).

Kinetic reduction curves (α vs t) of γ-Al_2O_3-supported iron catalysts were carried out at 520°C in H_2. From these kinetic curves both the initial reduction rate (r_0), determined by analytical differentiation of the integral kinetic data extrapolating at $t = 0$, and the reduction degree reached after 16 h (α_f) were obtained. These values are summarized in Table 1. Despite the scatter of the data an increase in r_0 with increasing Fe content may be observed. Nevertheless, the largest r_0 value [35.6 mg (g Fe)$^{-1}$ min^{-1}] corresponds to the 3IW sample. Similar behavior is observed when the reduction degrees reached after 16 h are compared with the r_0 values. The extent of reduction increases slightly as the protonation level of Al_2O_3 increases except for the PA20 sample for which a significant decrease in the α_f value is observed. For this sample a high dissolution of Al^{3+} ions, in the protonation step of Al_2O_3, is expected to take place. In this case, Fe^{3+} ions can isomorphically substitute Al^{3+} ions at the interface of alumina (*11, 21*). As a consequence, the catalyst becomes difficult to be reduced.

One can consider the reaction between iron and Al_2O_3 to produce $FeAl_2O_4$-like structures. It is well known that iron aluminate formed during the calcination step of the precursors is more difficult to reduce than bulk iron oxides (*22–24*). The same behavior was found in the case of cobalt (*24*) or nickel (*25, 26*) in alumina catalysts. In our case, the low α_f values obtained, even at 520°C after 16 h, are indicative of a strong interaction between the active phase and the carrier, presumably forming, to a certain extent, an iron aluminate–spinel phase. XRD measurements did not evidence the appearance of such a compound, probably owing to the fact that its formation may be restricted to only a few subsurface layers which can have a defined structure. Mössbauer results corroborate these findings (see below).

CO chemisorption. Figure 1 shows the pairs of CO isotherms obtained as described above for the NA, PA20, and 3IW samples. For each of the catalysts both isotherms are displaced by a constant CO uptake corresponding to the amount of strongly chemisorbed CO. The second isotherm must correspond to weakly chemisorbed CO on both support and unreduced Fe^{3+} ions as evidenced by the completely

TABLE 2

Dispersion Degree of Iron Particles and Activity of Fe/Al_2O_3 Catalysts

Catalyst	CO [mmole (g Fe)$^{-1}$]	S [m^2 (g Fe)$^{-1}$]	Dispersion (%)	Activity [μmole NH_3 (g Fe)$^{-1}$ h^{-1}]
NA	1.609	130.8	18.0	2.83
PA1	1.634	132.9	18.3	2.38
PA2.5	1.650	134.2	18.5	3.43
PA5	1.700	138.2	19.0	3.83
PA10	1.841	149.7	20.6	3.50
PA20	1.349	109.7	15.1	1.93
3IW	0.781	63.5	8.7	1.48
15IW	0.467	29.0	2.6	0.84

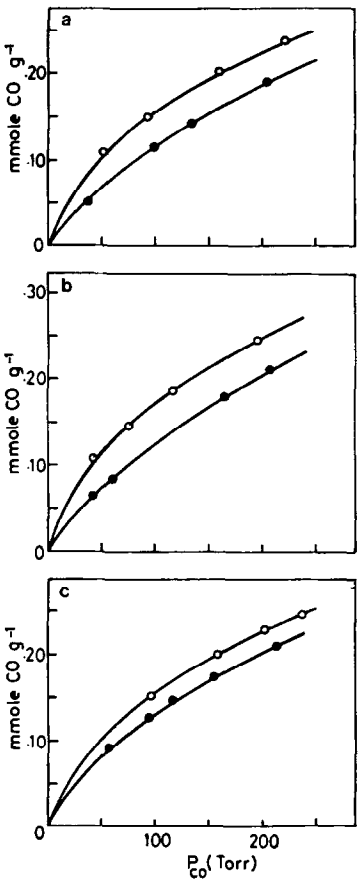

FIG. 1. CO adsorption isotherms at 195 K for several catalysts: (a) NA, (b) PA20, (c) 3IW. Open symbols, total amount of adsorbed CO. Solid symbols, amount of CO reversibly adsorbed upon the catalyst.

reversible CO uptake found on the oxidic IW sample. Thus, the difference between both isotherms represents the CO irreversibly chemisorbed on the metallic iron and possibly on Fe^{2+} ions. The irreversible CO uptakes [given as mmole CO (g Fe)$^{-1}$] are summarized in Table 2. As can be observed CO uptake increases progressively as the protonation level of the alumina surface increases, except for the PA20 sample in which it decreases. Even a smaller amount of CO was obtained on the IW samples.

From the assumed Fe/CO = 2/1 surface stoichiometry (*27*) and using a cross-sectional area per CO molecule of 0.135 nm, the metallic surface area (S) of Fe can be calculated (Table 2). In parallel, taking the same Fe/CO surface stoichiometry, the dispersion degree defined by the ratio Fe atoms at surface/total Fe atoms (%) can be calculated. As can be observed, the Fe dispersion follows a trend similar to that found for the Fe surfaces of the catalysts because of the small variation in the Fe content of the catalysts.

Variation of the Fe surface (or dispersion degree) with protonation of the γ-Al_2O_3 surface may be controlled by two factors. First, when the acid content of the support increases, the extent of adsorption of $[Fe(CN)_6]^{-4}$ ions must be favored (*13*); thus an increase in Fe loading is expected, although without significant differences in dispersion. Second, when the acid content of the support is high a fraction of the surface Al^{3+} ions might be isomorphically replaced by Fe^{3+} ions. In this matrix such ions would be difficult to reduce; consequently they would not irreversibly chemisorb CO molecules. This finding is also supported by the low degree of reduction found for PA20 catalyst (Table 1).

We recall that the degree of dispersion obtained from the irreversibly chemisorbed CO is certainly high for these catalysts. By using thermodesorption of CO from reduced iron-based catalysts, Perrichon *et al.* (*23*) found that a small fraction of adsorbed CO molecules were dissociated on Fe atoms. Such an effect could also be involved in the CO chemisorption experiments performed in this study. In this respect we used infrared spectroscopy to identify the adsorbed species formed after adsorption of NO on the 15% Fe/Al_2O_3 catalyst, 15IW (NO is considered to be a better probe molecule than CO to identify Fe atoms or ions).

X-Ray photoelectron spectra. Photoelectron spectra of the Fe $2p_{3/2}$ and Fe $2p_{1/2}$ levels of several Fe/Al_2O_3 catalysts are given in Fig. 2. The BE value of 711.0 eV was essentially the same for all catalysts, and the small differences of about 0.2 eV were within experimental error. Note that the BE value of Fe $2p_{3/2}$ level closely corresponds to that reported by Allen *et al.* (*28*),

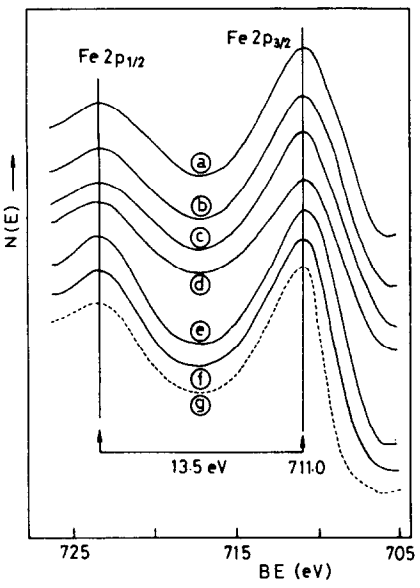

FIG. 2. Fe 2*p* peak profiles of oxidic catalysts. (a) NA, (b) PA1, (c) PA2.5, (d) PA5, (e) PA10, (f) PA20, (g) 3IW (dashed line).

Brundle *et al.* (*29*), and Yabe *et al.* (*30*) for the α-Fe_2O_3. The presence of α-Fe_2O_3 crystallites in these preparations (γ-Fe_2O_3 was excluded because no magnetic splitting is observed at room temperature) was evidenced by Mössbauer spectroscopy (see below). It is not surprising because the α-Fe_2O_3 is the more common Fe^{3+} oxide, with the more uniform corundum structure, in which the oxygen ions adopt a hexagonal close-packed arrangement and the Fe^{3+} ions are distributed throughout two-thirds of the octahedral sites generated in this structure.

No significant differences in the BE of O 1*s*, Al 2*p*, and K 2*p* photolines were observed, but their intensities varied substantially. In this respect, it is important to keep in mind that the intensities of the Fe 2*p* levels in Fig. 2 are not comparable because the number of accumulations also varied. As an approach to a better understanding of the dispersion of Fe and K species at the interface of these catalysts, the M 2*p*/Al 2*p* (M = Fe or K) ratios have been calculated and compared in Fig. 3 with the corresponding M/Al ratios as given by chemical analysis. For calculation of the M 2*p*/Al 2*p* ratio the sensitivity factors, averaged for different compounds and taking $f_{F1s} = 1.00$ as standard according to Wagner *et al.* (*31*), have been considered. As can be observed from Fig. 3, the surface concentration of Fe is much smaller than that corresponding to chemical analysis, while the one of K is about one-half of the overall composition. This fact suggests that the iron is dispersed inside the pores of the γ-Al_2O_3, while potassium is almost uniformly distributed on the surface. Moreover, the exposed Fe atoms at the surface increase slightly with Fe content. Thus, the small fraction of Fe atoms probed by XPS cannot be correlated with CO chemisorption or Mössbauer data. This small fraction of Fe could be related to those Al^{3+} ions of the γ-Al_2O_3 surface replaced isomorphically by Fe^{3+} ions during the impregnation step. On calcining, these Fe^{3+} ions should remain imbedded in the Al_2O_3 matrix.

Infrared spectra. The infrared spectra obtained after NO is chemisorbed on the oxidic and reduced alkali-promoted Fe/Al_2O_3 catalysts are given in Figs. 4A and B, respectively. We selected only the region 1900–1600 cm^{-1} characteristic of vibrations

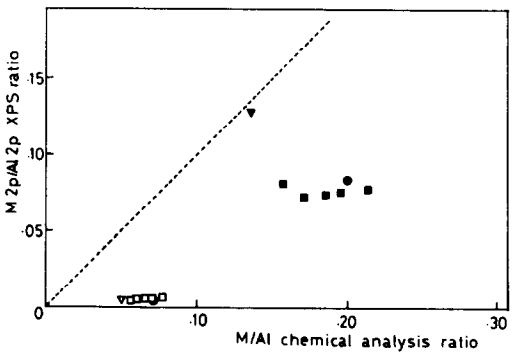

FIG. 3. XPS surface composition (M/Al, M = Fe or K) as a function of the chemical composition of different catalysts: ▽, NA; □, PA samples with variable protonation degree of the alumina (Table 1); ○, 3IW. Open and solid symbols refer to Fe and K, respectively. The dashed line is the theoretical one that would result if both surface and bulk compositions were identical.

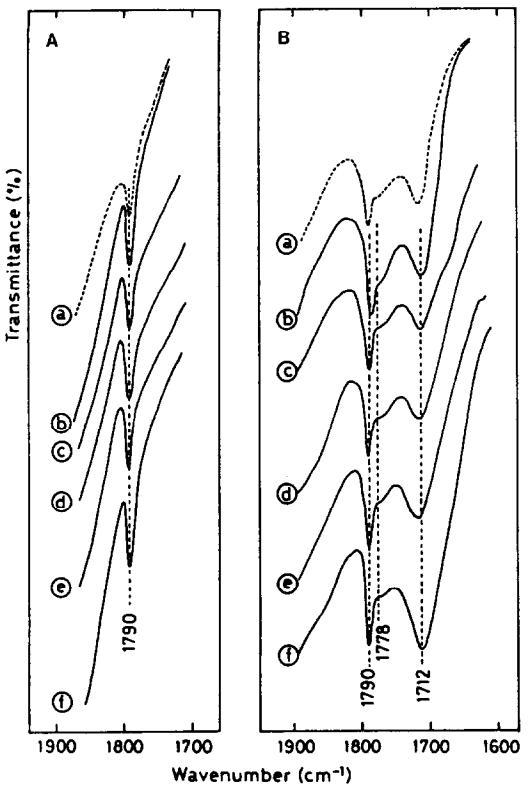

FIG. 4. Infrared spectra of NO chemisorbed (excess gas-phase NO) on (A) oxidic catalysts, and (B) reduced catalysts at 723 K for 2 h. (a) 3IW (dashed line), (b) NA, (c) PA2.5, (d) PA5, (e) PA10, (f) PA20.

of the NO probe held by ionic (or metallic) iron sites. For the oxidic catalysts (Fig. 4A), the spectra, obtained with the gas-phase NO (4.7 kN m^{-2}), show a very narrow band at 1790 cm^{-1} whose intensity is almost the same for all catalyst series, except for the 3IW catalyst which is slightly smaller. This band is completely removed upon evacuation of the cell to 1.7 N m^{-2}. The blank experiment did not show any IR bands.

NO chemisorption spectra on reduced catalysts show three bands at 1790, 1778 (shoulder), and 1712 cm^{-1}. In these reduced catalysts both the position and the full width at half-maximum (FWHM) of the band at 1790 cm^{-1} are almost the same as those found on the oxidic catalysts. Thus, it may be inferred that the surface species responsible for such a band is the same in both catalyst series. The relative intensity of the other two bands at 1778 and 1712 cm^{-1} depends markedly on the protonation degree of γ-Al_2O_3. For instance, the intensity of the band at 1778 cm^{-1} is higher than that at 1712 cm^{-1} for the NA catalyst while this trend is opposite for the PA20 catalyst.

Assignments of the infrared bands centered at 1800 and 1720 cm^{-1} have been made by Bandow *et al.* (*32*) by reacting NO with iron vapor and trapping the products by matrix isolation techniques. They assigned the band at 1800 cm^{-1} as monomeric NO species chemisorbed on Fe^{2+} sites, and a band at 1720 cm^{-1} as NO chemisorbed on fully reduced Fe^0 atoms. The Fe^{2+} sites were considered to be formed by oxidation of the Fe atoms by the NO probe molecule. These assignments were also made by King and Peri (*33*), who performed a careful infrared study of NO chemisorption upon alumina-supported iron and alkalinized iron Fischer–Tropsch catalysts, although they found a greater number of bands than observed by matrix isolation. No evidence was found supporting the formation of NO dimers in the matrix isolation experiments, in contrast to other studies of NO chemisorption on supported catalysts, namely, molybdena–alumina (*34*), chromia–alumina (*35*), and chromia–silica (*36, 37*).

In the present study the infrared bands of NO at 1778 and 1712 cm^{-1}, observed only on reduced catalysts, can reasonably be assigned to NO chemisorbed on Fe^{2+} and Fe^0 sites, respectively. Note that such bands appear slightly shifted to lower wavenumbers than those reported by Peri and King in an (up to 2%) alkali-supplemented 10% Fe/Al_2O_3 catalyst (*33*). The K-promoted iron catalysts of the present study show greater shifts owing to their higher promoter contents. Moreover, the greater alkali content resulted in a decrease of the band intensity, suggesting a loss of surface sites for NO chemisorption. By contrast, the band at 1790 cm^{-1} observed either on oxidized on reduced catalysts can be as-

signed to NO adsorbed on Fe^{3+} sites. This assignment is supported by the Mössbauer spectra which indicate the presence of only Fe^{3+} sites (see below). These Fe^{3+} sites are able to adsorb NO. Otto and Shelef (*38*) carried out a study on the equilibrium and kinetics of NO adsorption on Fe/Al_2O_3 catalysts. On the basis of a modelistic analysis of the NO isotherms (299–423 K) on 8.15% Fe/Al_2O_3 catalyst according to Freundlich's method, they found a value of 5.5 kcal $mole^{-1}$ for the adsorption heat (isosteric) at a NO coverage of 0.37. In agreement with the above statement, the NO coverage of the infrared species is expected to be rather high and also weak enough to exhibit a sharp infrared band. Therefore, the ionic Fe^{3+} sites, present on the oxidic and partially reduced catalysts, are presumably responsible for the infrared band of NO at 1790 cm^{-1}.

Mössbauer spectra. The Mössbauer spectra of the oxidic 15IW (for comparative purposes), 3IW, NA, and PA20 catalyst samples show nonmagnetic splitting and a broad doublet in the central region which was fitted to two doublets (Fig. 5). The results obtained are summarized in Table 3.

The strong double "A", with an isomer shift (IS) of 0.34 ± 0.03 mm s^{-1} and a quadrupole splitting (QS) of 0.62–1.00 mm s^{-1} is identified as due to superparamagnetic fine α-Fe_2O_3 particles (*39, 40, 42*). As the QS depends on the particle size of α-Fe_2O_3 (*39, 41–43*) the variation from 0.62 to 1.00 mm s^{-1} in the "A" doublet may be attributable to the variation of particle size from 12.0 to 5.0 nm in the samples. Large linewidths (Γ) of spectra are expected from supported iron oxide microcrystallites and may suggest the superimposition of different doublets arising from a heterogeneity of Fe^{3+} sites (*42*). The Mössbauer parameters of the second doublet "B" of weak intensity (Table 3) are characteristic of Fe^{2+}. The nature of this state has not been elucidated, as only ferric species are expected after the prolonged heating under an air flow. The fitting to a single doublet yields a large linewidth (Γ = 1.1 ± 0.3) with a very poor fit (χ^2/df = 1.5 ± 0.3).

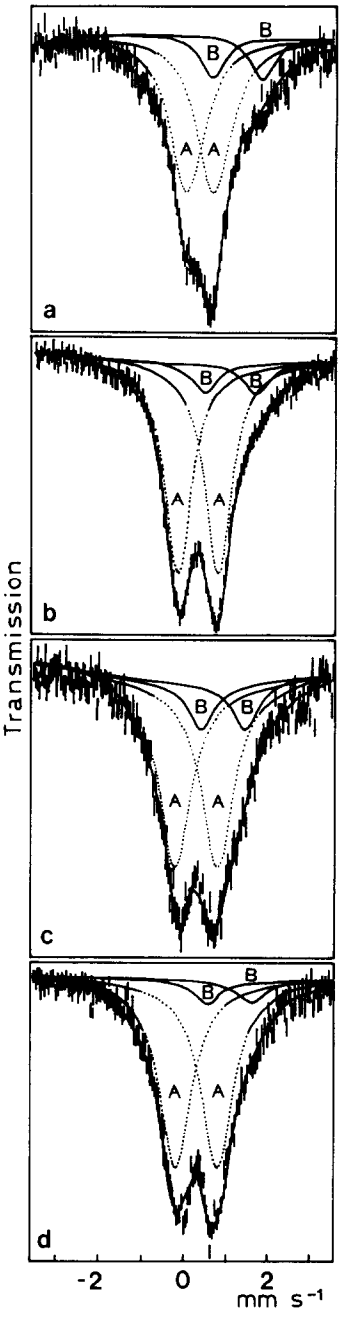

FIG. 5. Room temperature Mössbauer spectra of different alumina-supported iron catalysts: (a) 15IW, (b) 3IW, (c) NA, (d) PA20.

The Mössbauer spectra of the reduced samples show three different patterns (Fig. 6). The spectrum of sample 15IW consists

TABLE 3

Mössbauer Parameters of Unreduced Catalyst Samples
(IS Relative to α-Fe)

	15IW	3IW	NA	PA20
Fe^{3+} (A)				
QS (mm s^{-1})	0.62 ± 0.07	0.94 ± 0.01	1.00 ± 0.02	0.97 ± 0.02
IS (mm s^{-1})	0.38 ± 0.04	0.35 ± 0.01	0.31 ± 0.02	0.32 ± 0.02
Γ (mm s^{-1})	0.99 ± 0.02	0.76 ± 0.02	0.90 ± 0.06	0.93 ± 0.04
I_A/I_{tot}	0.84 ± 0.07	0.88 ± 0.02	0.84 ± 0.08	0.92 ± 0.04
Fe^{2+} (B)				
QS (mm s^{-1})	1.16 ± 0.05	1.21 ± 0.05	1.06 ± 0.07	1.05 ± 0.11
IS (mm s^{-1})	1.24 ± 0.03	1.12 ± 0.03	0.94 ± 0.04	1.11 ± 0.06
Γ (mm s^{-1})	0.70[a]	0.70[a]	0.70[a]	0.70[a]
I_B/I_{tot}	0.16 ± 0.04	0.12 ± 0.01	0.16 ± 0.03	0.08 ± 0.01
χ^2/df[b]	1.00	1.06	1.00	1.42

[a] The value of the parameter was constrained in the fit.
[b] df = degrees of freedom.

of two magnetic sextets (one of α-Fe and another corresponding to α-Fe_2O_3 in the form of small particles (*40*)), one doublet assigned to Fe^{3+}, and a single peak in the center of the spectrum, with a very weak intensity attributable to superparamagnetic Fe^0 (*43–45*). The inclusion of this peak in the fitting slightly improves the goodness of fit.

The spectra of samples 3IW and NA show the α-Fe sextet, the single center peak of superparamagnetic Fe^0, and two doublets assigned to Fe^{2+} and Fe^{3+}. The sextet of α-Fe is not visible in the spectrum of sample PA20 and its central region contains superparamagnetic Fe^0, Fe^{2+}, and Fe^{3+} as the spectra from 3IW and NA. The fitting spectra given in Fig. 6 yield the Mössbauer parameters presented in Table 4, which also contain the relative concentrations of the different species in the spectra. The central region of spectra from reduced samples is poorly resolved and leaves much freedom for computer fitting. A large linewidth for the Fe^{2+} doublet has frequently been observed for spectra of supported iron catalysts (*44*) and attempts to fit two Fe^{2+} doublets did not improve significantly, if at all, the statistics of the fit.

In agreement with Berry (*42*), sample 15IW with the highest iron content is the one most easily reduced to metal iron. A high ferric oxide concentration may result in the iron atoms being less intimately bonded to the support, and more readily reducible to Fe^0.

Catalytic Activity

In this work, catalytic activity for ammonia synthesis was correlated with the surface characteristics of the catalysts and their method of preparation (see Table 2).

Catalysts NA, PA1, PA2.5, PA5, PA10, PA20, 3IW, and 15IW were used to study catalytic activities for ammonia synthesis at atmospheric pressure. Figure 7 shows increasing catalytic activity with increasing acid content of γ-Al_2O_3, reaching a maximum value for catalysts between PA5 and PA10. Catalysts with an acid content of γ-Al_2O_3 higher than 10 mmole H^+ (g Al_2O_3)$^{-1}$ (PA10) show a rapid decrease in their catalytic activity, probably due to a change in the surface structure of the catalyst with increasing protonation of the γ-Al_2O_3, as shown by decreases in the reduction degree, α_f (Table 1), and dispersion (Table 2), going from PA10 to PA20 catalysts.

TABLE 4

Mössbauer Parameters of Reduced Catalyst Samples (IS Relative to α-Fe)

	15IW	3IW	NA	PA20
α-Fe				
QS (mm s^{-1})	0[a]	0[a]	0[a]	
IS (mm s^{-1})	−0.04 ± 0.03	0.06 ± 0.02	0.01 ± 0.02	
H (kG)	332. ± 1.	331. ± 1.	335. ± 1.	—
Γ (mm s^{-1})	0.34 ± 0.01	0.31 ± 0.05	0.25 ± 0.05	
$I_{\alpha\text{-Fe}}/I_{tot}$	0.39 ± 0.01	0.04 ± 0.01	0.08 ± 0.01	
Fe_s^0 (superparamagnetic)				
QS (mm s^{-1})	0[a]	0[a]	0[a]	0[a]
IS (mm s^{-1})	0.09 ± 0.04	0.02 ± 0.02	−0.07 ± 0.02	0.01 ± 0.01
Γ (mm s^{-1})	0.24 ± 0.08	0.51 ± 0.06	0.95 ± 0.22	0.54 ± 0.05
$I_{Fe_s^0}/I_{tot}$	0.01 ± 0.001	0.17 ± 0.04	0.11 ± 0.07	0.25 ± 0.03
$Fe^0 = -Fe + Fe_s^0$				
I_{Fe^0}/I_{tot}	0.40 ± 0.01	0.21 ± 0.04	0.19 ± 0.07	0.25 ± 0.03
Fe^{2+}				
QS (mm s^{-1})		1.29 ± 0.05	1.44 ± 0.08	1.08 ± 0.06
IS (mm s^{-1})		1.12 ± 0.03	0.96 ± 0.04	1.30 ± 0.05
Γ (mm s^{-1})	—	0.90 ± 0.02	0.98 ± 0.05	1.13 ± 0.09
$I_{Fe^{2+}}/I_{tot}$		0.49 ± 0.03	0.54 ± 0.06	0.53 ± 0.05
Fe^{3+}				
QS (mm s^{-1})	0.73 ± 0.01	1.92 ± 0.01	0.84 ± 0.02	0.95 ± 0.05
IS (mm s^{-1})	0.28 ± 0.03	0.25 ± 0.02	0.25 ± 0.02	0.17 ± 0.02
Γ (mm s^{-1})	0.65 ± 0.02	0.52 ± 0.02	0.45 ± 0.06	0.54 ± 0.06
$I_{Fe^{3+}}/I_{tot}$	0.51 ± 0.01	0.30 ± 0.04	0.27 ± 0.07	0.22 ± 0.04
$\alpha\text{-}Fe_2O_3$				
QS (mm s^{-1})	−0.16 ± 0.03			
IS (mm s^{-1})	0.36 ± 0.03			
H (kG)	530. ± 1.	—	—	—
Γ (mm s^{-1})	0.30 ± 0.04			
$I_{\alpha\text{-}Fe_2O_3}/I_{tot}$	0.09 ± 0.04			
χ^2/df[b]	1.55	2.30	1.94	1.01

[a] The value of the parameter was constrained in the fit.
[b] df = degrees of freedom.

Figure 7 also plots the catalytic activities versus iron content of the catalysts. This figure compares the catalytic activities of catalysts prepared from the incipient wetness impregnation method (IW) with those of catalysts prepared by the "free adsorption" method. The results show that at comparable iron contents, the catalytic activity of the PA5 catalyst is double that of the 3IW catalyst and four times that of 15IW.

Consequently, the catalytic activities [given in $(g\ Fe)^{-1}$] of these catalysts depend on the surface characteristics of the active phase and consequently on the acid modification of $\gamma\text{-}Al_2O_3$ and impregnation method used.

The importance of surface potassium may be found from XPS results in Fig. 3, which depicts the NA catalyst as having all the potassium on the surface. This fact may account for its higher activity when com-

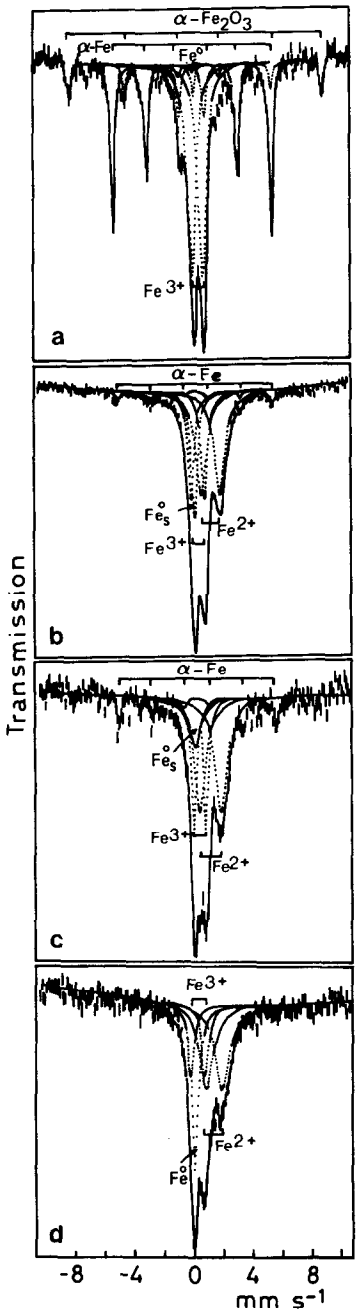

FIG. 6. Room temperature Mössbauer spectra of different reduced catalyst samples: (a) 15IW, (b) 3IW, (c) NA, (d) PA20.

pared with PA20, 3IW, and 15IW catalysts with higher iron content but different surface structure of the iron particles.

The data obtained from Mössbauer spectra should be more reliable than those obtained from reduction measurements. However, these Mössbauer results tell us very little about the content of crystallographic planes responsible for the active sites in a "structure sensitive" catalyst. So, we should not expect to account for the activity values obtained on the basis of Mössbauer data alone. On the other hand, activity values correlate well with iron dispersion data, suggesting that the active sites are located mainly within the pores of the catalyst, as determined by CO chemisorption measurements.

CONCLUSIONS

Several iron catalysts supported on γ-Al_2O_3 and prepared by two methods of impregnation, the "incipient wetness" and the free adsorption" methods, showed the following characteristics: (1) The iron is well dispersed within the pores of the support, as determined by CO chemisorption, and potassium is dispersed mainly on the surface according to XPS results. (2) Fe^0 surface content increased with protonation pretreatment of γ-Al_2O_3, as determined by IR with NO as probe molecule. Mössbauer spectra, and also IR spectra, showed the presence of Fe^{2+} in the reduced catalysts, and quantified all the reduced and unre-

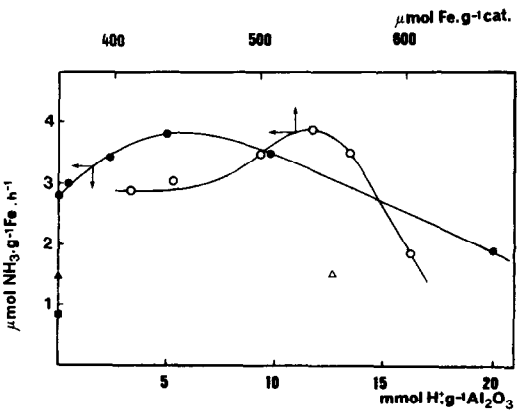

FIG. 7. Plots of catalytic activity vs acid modification of the support (solid symbols), and vs iron content of the catalyst (open symbols), for the following Fe/Al_2O_3 catalysts: ○, NA and PA; △, 3IW; □, 15IW.

duced iron species. Mössbauer spectra show a decreasing fraction of small superparamagnetic Fe_s^0 particles with iron loading, for "incipient wetness" catalysts, and an increasing fraction of those with protonation of γ-Al_2O_3, for "free adsorption" catalysts.

The activity of these catalysts [expressed as $(g\ Fe)^{-1}$] in ammonia synthesis at atmospheric pressure and 350°C showed that (1) "free adsorption" catalysts, especially those with a certain protonation pretreatment of γ-Al_2O_3, were more active than those prepared by the "incipient wetness" method, and (2) activity values correlate well with iron dispersion data suggesting that the active sites are located within the pores of the catalysts rather than on their surface, according to CO chemisorption and XPS results.

REFERENCES

1. Ozaki, A., Aika, K., and Hori, H., *Bull. Chem. Soc. Japan* **44,** 3216 (1971).
2. Takezawa, N., Toyoshima, I., and Suzuki, H., *Z. Phys. Chem. (Frankfurt)* **89,** 323 (1974).
3. Ozaki, A., and Aika, K., "Catalysis, Science and Technology," Part I, Chap. 3. Springer-Verlag, Berlin, 1981.
4. Nielsen, A., *Catal. Rev. Sci. Eng.* **23,** 17 (1981).
5. Peri, J. B., *J. Phys. Chem.* **70,** 1482 (1966).
6. Brunelle, J. P., and Sugier, C. E., *C.R. Acad. Sci. Ser. C* **276,** 1545 (1973).
7. Jirátová, K., and Beránek, L., *Appl. Catal.* **2,** 125 (1982).
8. Brunelle, J. P., *Pure Appl. Chem.* **50,** 1211 (1978).
9. D'Aniello, M. J., Jr., *J. Catal.* **69,** 9 (1981).
10. Homs, N., Ramírez de la Piscina, P., and Sueiras, J. E., *J. Catal.* **89,** 531 (1984).
11. Fierro, J. L. G., Homs, H., Ramírez de la Piscina, P., and Sueiras, J. E., *Z. Phys. Chem. N. F.* **135,** 235 (1983).
12. Fierro, J. L. G., Homs, N., Ramírez de la Piscina, P., and Sueiras, J. E., *React. Kinet. Catal. Lett.* **24,** 179 (1984).
13. Homs, N., Ramírez de la Piscina, P., Fierro, J. L. G., and Sueiras, J. E., *Z. Anorg. Allg. Chem.* **518,** 227 (1984).
14. Ramírez de la Piscina, P., Homs, N., and Sueiras J. E., *Z. Anorg. Allg. Chem.* **522,** 235 (1985).
15. Ramírez de la Piscina, P., Homs, N., Fierro, J. L. G., and Sueiras, J. E., *Z. Anorg. Allg. Chem.* **528,** 195 (1985).
16. Homs, N., Ramírez de la Piscina, P., Fierro, J. L. G., and Sueiras, J. E., *Z. Anorg. Allg. Chem.*, in press.
17. Chaney, A. L., and Marbach, E. P., *Clin. Chem.* **8,** 130 (1962).
18. Emmett, P. H., and Brunauer, S. J., *J. Amer. Chem. Soc.* **56,** 351 (1934).
19. Emmett, P. H., and Harkness, R. W., *J. Amer. Chem. Soc.* **57,** 1631 (1935).
20. Emmett, P. H., and Brunauer, S. J., *J. Amer. Chem. Soc.* **59,** 1553 (1937).
21. Lund, C. R. F., and Dumesic, J. A., *J. Phys. Chem.* **85,** 3175 (1981).
22. Brown, R., Cooper, M. E., and Whan, D. A., *Appl. Catal.* **3,** 177 (1982).
23. Perrichon, V., Charcosset, H., Barrault, J., and Forquy, C., *Appl. Catal.* **7,** 21 (1983).
24. Smith, P. J., Taylor, D. W., Dowden, D. A., Kemball, C., and Taylor, D., *Appl. Catal.* **3,** 303 (1982).
25. Gambaro, L. A., Fierro, J. L. G., González Tejuca, L., and López Agudo, A., *Surf. Int. Anal.* **4,** 234 (1982).
26. Gajardo, P. Grange, P., and Delmon, B., *J. Chem. Soc. Faraday Trans.* **77,** 665 (1980).
27. Boudart, M., Delbouille, A., Dumesic, J. A., Khammouma, S., and Topsøe, H., *J. Catal.* **37,** 486 (1975).
28. Allen G. C., Tucker, P. M., and Wild, R. K., *Philos. Mag. B* **46,** 411 (1982).
29. Brundle, C. R., Chang, T. J., and Wandelt, K., *Surf. Sci.* **459** (1977).
30. Yabe, K., Arata, K., and Toyoshima, I., *J. Catal.* **57,** 231 (1979).
31. Wagner, C. D., Davis, L. E., Zeller, M. V., Taylor, J. A., Raymond, R. H., and Gale, L. H., *Surf. Int. Anal.* **3,** 211 (1981).
32. Bandow, H., Onishi, T., and Tamaru, K., *Chem. Lett.*, 83 (1978).
33. King, D. L., and Peri, J. B., *J. Catal.* **79,** 164 (1983).
34. Yao, H. C., Rothschild, W. G., and Gandhi, H. S., "Catalysis on the Energy Scene" (S. Kaliaguine and A. Mahay, Eds.), p. 71. Elsevier, Amsterdam, 1984.
35. Peri, J. B., *J. Phys. Chem.* **78,** 588 (1974).
36. Zecchina, A., Garrone, E., Morterra, C., and Colluccio, S., *J. Phys. Chem.* **79,** 978 (1975).
37. Kugler, E. L., Kokes, R. J., and Gryder, J. W., *J. Catal.* **36,** 142 (1975).
38. Otto, K., and Shelef, M., *J. Catal.* **18,** 184 (1970).
39. Yoshioka, T., Koezuka, J., and Ikoma, H., *J. Catal.* **16,** 264 (1970).
40. Künding, W., Bömmel, H., Constabaris, G., and Lindquist, R. H., *Phys. Rev.* **142,** 327 (1966).
41. Künding, W., Ando, K. J., Lindquist, R. H., and

Constabaris, G., *Czech. J. Phys. B* **17,** 467 (1967).
42. Berry, F. J., *in* "Advances in Inorganic Chemistry and Radiochemistry" (H. J. Emeleus and A. G. Sharpe, Eds.), Vol. 21, p. 255. Academic Press, New York, 1978.
43. Topsøe, H., Dumesic, J. A., and Mørup, S., *in* "Applications of Mössbauer Spectroscopy" (R. L. Cohen, Ed.), Vol. 2, p. 56. Academic Press, New York, 1980.
44. Niemantsverdriet, J. W., Van der Kraan, A. M., Delgass, W. N., and Vannice, M. A., *J. Phys. Chem.* **89,** 67 (1985).
45. Boudart, M., Delbouille, A., Dumesic, J. A., and Topsøe, H., *J. Catal.* **37,** 486 (1975).